Synthesis and Structure–Property Relationships of Processable Liquid Crystalline Polymers with Arylenevinylene Segments in the Main Chain for Light-Emitting Applications

J. Oberski, R. Festag, C. Schmidt, G. Lüssem, J. H. Wendorff, and A. Greiner*

Fb Physikalische Chemie/Polymere und Wissenschaftliches Zentrum f. Materialwissenschaften, Philipps-Universität Marburg, Hans-Meerwein-Strasse, Geb. H, 35032 Marburg, Germany

M. Hopmeier

Fb Physik, Philipps-Universität Marburg, Am Renthof 5, 35032 Marburg, Germany

F. Motamedi

Materials Department, University of California–Santa Barbara, Santa Barbara, California 93106

Received May 25, 1995; Revised Manuscript Received August 31, 1995[⊗]

ABSTRACT: Polymers were synthesized with modified *trans*-bis(styryl)benzene segments in the main chain by polycondensation of OH-functionalized oligo(arylenevinylenes) and aliphatic diacid chlorides. Most of the visible light emitting polymers were soluble at room temperature and fusible below the range of decomposition. The formation of a smectic A phase was observed in the melt state. Isotropization temperatures of polymers with phenyl-substituted arylenvinylene segments were detected below 200 °C. A remarkable thermal stability in the melt state with respect to cross-linking was observed for polymers containing CF_3-substituted arylenevinylene segments. The polymers were investigated by spectroscopic methods, thermogravimetrical analysis, differential scanning calorimetry, polarizing microscopy, wide angle X-ray scattering, small angle X-ray scattering, dielectric relaxation spectroscopy, and by stress–strain experiments.

Introduction

The main chain of poly(1,4-phenylenevinylene) (PPV) is composed of an alternating sequence of phenylene and vinylene segments. The polymer is rodlike when the phenylene segments are in the trans position on the vinylene segments and it is then potentially liquid crystalline. However, PPV cannot form mesogenic phases since it is insoluble and infusible below the temperature range of decomposition, which is a major limitation for applications of PPV. Derivatives of PPV with modified arylenevinylene segments, mostly by lateral substitution, exhibit thermotropic LC behavior but the LC phases are unstable due to the thermally induced cross-linking reaction.[1] The same phenomena were observed by Saegusa et al. for polymers with bis(styryl)benzene segments and aliphatic spacers in the main chain.[2] Karasz et al. prepared polymers composed of ethylene oxide segments and substituted bis(styryl)benzene segments in the main chain which did not exhibit any indication for LC behavior.[3] These materials have been used successfully as light emitters in LED devices. Following a similar concept, Schmidt et al. investigated copolyesters containing isolated dinaphthylenevinylene units for LED applications.[4] Blue photoluminescence was found with dialkoxy-substituted bis(styryl)benzene segments and dioxyalkylene spacers in the main chain. Liquid crystallinity was claimed for this polymer.[5]

In the past we have studied the blending behavior of soluble poly(arylenevinylenes),[6] the blending behavior of bis(styryl)benzenes,[7] the electroluminescent behavior of these materials,[8] and the preparation as well as the electroluminescence of polymers with arylenvinylene segments in the side chains.[9] The present paper is focused on the synthesis and properties of polymers with well-defined arylenevinylene segments in the main chain.[10] The objective is the preparation of liquid crystalline visible light emitting soluble polymers for optical applications. The solubility is an essential prerequisite to prepare high-quality films for optical applications. The LC character of these polymers will allow orientation on a molecular level of the light-emitting polymers. The combination of light emission and order on a molecular level is a promising concept for new optical applications. The luminescence properties will be discussed here just briefly but are the topic elsewhere.[11]

Experimental Part

Materials. $Pd(OAc)_2$ was used as received (Degussa). Tri-*o*-tolylphosphine was synthesized according to ref 12. DMF was distilled over 4,4′-methylenebis(phenyl isocyante). Triethylamine was distilled over KOH. *p*-Acetoxystyrene was used as received (Hoechst). 2,5-Dibromo-*p*-xylene (Aldrich), 2,5-dibromonitrobenzene (Aldrich), and 2,5-dibromo(trifluoromethyl)benzene (Alfa) was used as received. 1,4-Dibromo-1,4-dimethoxybenzene[13] and 2,5-dibromobiphenyl[14] were prepared as reported previously. The aliphatic diacid chlorides were obtained by reaction of the corresponding aliphatic diacids (Aldrich) with thionyl chloride. Toluene was purified by distillation over sodium.

Measurements. NMR spectra were obtained on a Bruker AC 300. Thermogravimetrical analysis (TGA) was done on a Mettler TG 50/TC10. DSC was performed on a Perkin-Elmer DSC-VII. Polarizing microscopy was performed on a Leitz Orthoplan microscope. Viscosimetry was done on a Schott Automatic Viscosimeter AVS 400 and with Ubbelohde type viscosimeters. The X-ray analysis was performed using a wide angle diffractometer (Siemens D 5000, with Ni filter) and a flat camera as well as a small angle Kratky compact camera.

[⊗] Abstract published in *Advance ACS Abstracts,* November 1, 1995.

0024-9297/95/2228-8676$09.00/0

Table 1. Reaction Parameters for the Preparation of 1,4-Bis(*p*-acetoxystyryl)benzenes 3

code	react. temp, °C	react time, h	recrystal. from	yield, %
3a	110	48	toluene	92
3b	100	36	petrol ether	96
3c	120	96	toluene	68
3d	110	72	toluene	86
3e	120	96	toluene	60

Dielectric relaxation spectroscopy was performed on a Hewlett Packard model 4284 A Precision LCR meter.[15] Mechanical tests were performed on an Instron tensile tester (model 1122). Fibers were produced by pulltrusion on a hot plate. Photoluminescence spectra were recorded at 13 K by a multichannel analyzer with an integration time of 682.4 μs and a slit width of 0.5 nm. Excitation was done by a Pyridin 2 dye laser at 360 nm with a repetition rate of 76 MHz and a pulse duration of <8 ps.

General Procedure for the Preparation of 1,4-Bis(*p*-acetoxystyryl)benzenes 3. A 250 mL three-necked glass flask equipped with a reflux condenser, a Stutz type check valve, an argon inlet, and a stirring bar was charged under an argon atomosphere with 50.0 mmol of dibromoarene, 105.0 mmol of *p*-acetoxystyrene (15.77 g), 110.0 mmol of triethylamine (11.13 g), 0.5 mmol of $Pd(OAc)_2$ (0.112 g), 3.0 mmol of tri-*o*-tolylphosphine (0.913 g), and 90 mL of DMF. The mixture was stirred and heated (temperatures and times are given in Table 1). The mixture was filtered after cooling, and the solid residue was rinsed with DMF. The filtrates were purged into 1.5 L of 2 N HCl. The solid product was isolated by filtration, washed with water, recrystallized, and dried in vacuum.

Details of the synthesis and characterization of the 1,4-bis(*p*-acetoxystyryl)benzenes **3** are given respectively in Tables 1 and 2.

General Procedure for the Preparation of 1,4-Bis(*p*-hydroxystyryl)benzenes 4. A 250 mL three-necked glass flask equipped with a reflux condenser, a Stutz type check valve, an argon inlet, and a stirring bar was charged under an argon atomosphere with 250.0 mmol of potassium hydroxide dissolved in 100 mL of methanol and 25.0 mmol of **3**. The mixture was refluxed for 3 h. The resulting clear solution was filtered after cooling. The filtrate was dropped into 2 L of 2 N HCl. The solid product was isolated by filtration and washed twice with water. Water was removed by dissolving the product in water followed by azeotropic distillation of water/toluene. The product recrystallized upon cooling of the toluene solution.

Details of the characterization of **4** are presented in Table 3.

Polymerization. A 100 mL three-necked flame-dried glass flask equipped with a reflux condenser, a Stutz type check valve, an argon inlet, and a stirring bar was charged under an argon atomosphere with 3.0 mmol of an aliphatic diacid chloride, 3.0 mmol of **4**, and 20 mL of a solvent. The mixture was stirred at the given temperature for the given time. After cooling to room temperature, the reaction mixture was dropped into ligroin. The solid product was filtered off, washed with ligroin, reprecipitated, and dried in vacuum. Details of the polymer preparation and the characterization data of **6** are given in Tables 4 and 5.

Results and Discussion

Monomer Synthesis. The OH-functionalized oligo(arylenevinylenes) with the general structure **4** were synthesized by Pd-catalyzed coupling of *p*-acetoxystyrene and p-dibromoarenes to form compounds **3** and subsequent hydrolysis of the acetoxy groups by base treatment, as shown in Scheme 1.

The chemical structure and purity of **3** and **4** was established by elemental analysis, IR, ^{1}H-NMR, and ^{13}C-NMR spectroscopy (Tables 2 and 3).

Polymer Synthesis. Polycondensation of equimolar amounts of **4** and **5** was carried out in solution, as indicated in Scheme 2 and Table 4, respectively. The choice of the solvent was related to the solubility of **4**. **6** was obtained in good yields. Inherent viscosities were measured between 0.11 and 0.5 dL/g. Molecular weights obtained were high enough to produce free-standing films by solution casting. The chemical structures of the polymers were verified by elemental analysis, IR spectroscopy, ^{1}H-NMR spectroscopy, and UV spectroscopy (Table 5).

The solubilities of the polymers depend significantly on the substituents at the central phenylene ring and the number of methylene groups in the diacid segment. All of the polymers are soluble in 1,1,2,2-tetrachloroethane at room temperature with the exception of polymer **6d**. The polymers **6g**, **6h**, **6i**, and **6k** are soluble in chloroform at room temperature. This improved solubility is obviously due to the longer aliphatic spacers. The enhanced solubility of **6h** and **6k** versus **6j**, **6l**, and **6m** has to be attributed to the substituents at the phenylene rings in the arylenevinylene segments. In comparison, polymers formed by polycondensation of linear aliphatic diols and stilbene-4,4′-dicarboxylates are insoluble.[16]

Thermal Properties of the Polymers (TGA, DSC, PM, X-ray, and DRS). Thermogravimetrical Analysis (TGA). The thermal stability of the polymers was

Table 2. Characterization Data for Compounds 3

code, formula	analysis, % calcd (found) C	H	T_m,[a] °C	^{1}H-NMR chemical shifts,[b] ppm	IR spectra wavenumber, cm^{-1}	UV spectra[c] λ_{max}, nm	ϵ, mg^{-1} cm^2
3a, $C_{32}H_{26}O_4$	80.99 (80.09)	5.52 (5.54)	182	2.31 (s, 3H), 2.35 (s, 3H), 7.03–7.55 (m, 20H)	3020 (w), 1757 (vst), 1506 (st), 1366 (m), 1191 (vst), 967 (st), 909 (st)	358	70
3b,[d] $C_{27}H_{21}F_3O_4$	69.52 (69.56)	4.54 (4.67)	139	2.34 (s, 6H), 7.08–7.79 (m, 15H)	3034 (w), 1762 (vst), 1508 (st), 1367 (m), 1197 (vst), 1157 (vst), 1115 (vst), 1050 (m), 969 (m), 913 (m), 840 (m)	355	163
3c,[e] $C_{26}H_{21}NO_6$	70.42 (70.30)	4.77 (4.94)	170	2.26 (s, 6H), 7.05–8.1 (m, 15H)	3027 (w), 1761 (vst), 1506 (st), 1364, 1194 (vst), 1014 (st), 969 (m)	342	44
3d, $C_{28}H_{26}O_4$	78.85 (78.57)	6.14 (6.02)	236	2.33 (s, 6H), 2.44 (s, 6H), 6.98–7.04 (d, 2H), 7.08–7.12 (d, 4H), 7.43 (s, 2H), 7.52–7.55 (d, 4H)	3056 (w), 3022 (w), 2967 (w), 2922 (w), 1760 (vst), 1507 (st), 1366 (m), 1119 (vst), 982 (st), 820 (m)	356	110
3e, $C_{28}H_{26}O_6$	73.35 (73.55)	5.72 (5.63)	231	2.26 (s, 6H), 3.87 (s, 6H), 7.01–7.05 (d, 4H), 7.07 (s, 4H), 7.35 (s, 1H), 7.41 (s, 1H), 7.49–7.51 (d, 4H)	3035 (w), 3002 (w), 2933 (w), 2826 (w), 1758 (vst), 1507 (st), 1365 (m), 1192 (vst), 1040 (st), 971 (s), 861 (st)	326 389	56

[a] T_m = melting point; measured by DSC (heating rate 10 °C/min). [b] ^{1}H-NMR spectra were measured in $CDCl_3$. [c] UV/vis spectra were measured in THF. [d] Elemental analysis for **3b** (fluorine): calcd, 12.22%; found, 12.38%. [e] Elemental analysis for 3c (nitrogen): calcd, 3.16%; found, 3.23%.

Table 3. Characterization Data for Compounds 4

code, formula	analysis, % calcd (found) C	H	T_m,[a] °C (yield, %)	^{1}H-NMR chemical shifts,[b] ppm	IR spectra wavenumber, cm^{-1}	UV spectra[c] λ_{max}, nm	ϵ, mg^{-1} cm^2
4a, $C_{28}H_{22}O_2$	86.13 (86.28)	5.68 (5.66)	132 (98)	4.89 (s, 2H), 6.70–7.66 (m, 26H)	3261 (m), 3022 (w), 1605 (st), 1511 (vst), 1170 (st), 960 (m)	369	184
4d,[d] $C_{23}H_{17}F_3O_2$	72.25 (72.09)	4.48 (4.55)	199 (99)	5.52 (s, 2H), 6.81–7.73 (m, 15H)	3265 (m), 3022 (w), 1605 (st), 1513 (vst), 1239 (vst), 1117 (vst), 1050 (m), 961 (m), 834 (m)	372	174
4c,[e] $C_{22}H_{17}NO_4$	73.53 (73.63)	4.77 (4.90)	217 (99)	6.60–8.26 (m, 15H), 9.67 (s, 1H), 9.72 (s, 1H)	3354 (m), 3016 (w), 1603 (st), 1512 (vst), 1346 (st), 1239 (st), 1172 (st), 962 (m), 837 (m)	357	111
4d, $C_{24}H_{22}O_2$	84.18 (84.28)	6.48 (6.36)	277 (99)	2.39 (s, 6H), 6.79–6.82 (d, 4H), 7.02–7.08 (d, 2H), 7.13–7.19 (d, 2H), 7.46–7.47 (d, 4 H), 7.48 (s, 2H), 9.60 (s, 2H)	3294 (m), 3015 (w), 2921 (w), 1590 (st), 1510 (vst), 1238 (sst), 1168 (st), 958 (st), 852 (st), 809 (st)	364	161
4e, $C_{24}H_{22}O_4$	76.99 (76.98)	5.92 (5.90)	302 (95)	3.81 (s, 6H), 6.68–6.78 (d, 4H), 7.14 (s, 4H), 7.32–7.42 (d, 4H), 9.60 (s, 2H)	3362 (m), 3068 (w), 3005 (w), 2948 (w), 1605 (st), 1514 (vst), 1260 (vst), 1197 (vst), 1172 (st), 1023 (vst), 958 (vst), 859 (st), 819 (st)	394, 325	123

[a] T_m = melting point; measured by DSC (heating rate 10 °C/min). [b] ^{1}H-NMR spectra were measured in $CDCl_3$ with the exception of **4c** and **d** which were measured in DMSO-d_6. [c] UV/vis spectra were measured in THF. [d] Elemental analysis for **4b** (fluorine): calcd, 14.91%; found, 15.23%. [e] Elemental analysis for **4c** (nitrogen): calcd, 3.90%; found, 3.92%.

Scheme 1

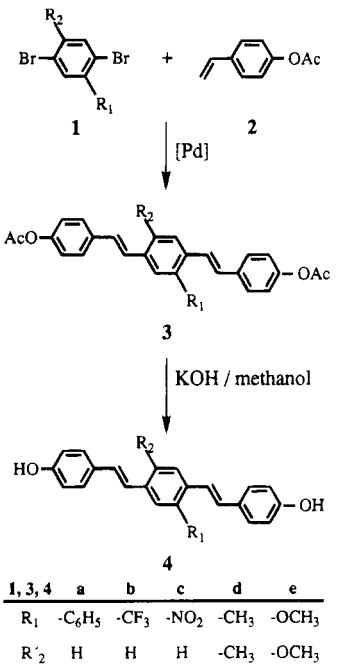

1, 3, 4	a	b	c	d	e
R_1	$-C_6H_5$	$-CF_3$	$-NO_2$	$-CH_3$	$-OCH_3$
R'_2	H	H	H	$-CH_3$	$-OCH_3$

Table 4. Reaction Parameters and Yields for Polymers 6

code	solvent	react. temp, °C	react. time, h	yield, %
6a	biphenyl	160	150	85
6b	biphenyl	155	120	90
6c	biphenyl	155	120	92
6d	toluene	120	120	95
6e	biphenyl	145	96	96
6f	xylene	135	96	89
6g	toluene	120	120	90
6h	toluene	120	80	88
6i	toluene	120	75	95
6j	xylene	135	140	82
6k	xylene	135	140	82
6l	biphenyl	160	150	89
6m	toluene	120	170	92

tested by heating under nitrogen between 50 and 800 °C with a heating rate of 20 °C/min and measuring the weight loss (TGA). All polymers exhibit single-staged

Scheme 2

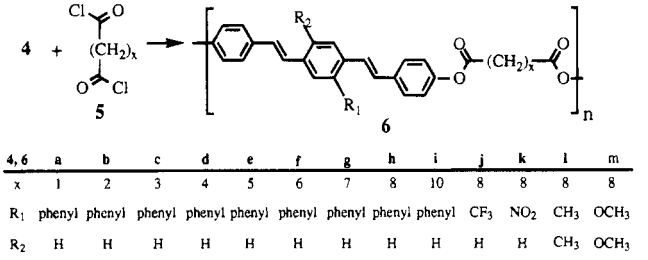

4, 6	a	b	c	d	e	f	g	h	i	j	k	l	m
x	1	2	3	4	5	6	7	8	10	8	8	8	8
R_1	phenyl	phenyl	phenyl	phenyl	phenyl	phenyl	phenyl	phenyl	phenyl	CF_3	NO_2	CH_3	OCH_3
R_2	H	H	H	H	H	H	H	H	H	H	H	CH_3	OCH_3

TGA traces with the exception of the NO_2-substituted polymer **6k**. For most of the polymers the 5% weight loss was detected close to 400 °C with inflection points around 460 °C (Table 6). Yet, TGA is not sufficient for measuring the thermal stability of polymers since degradation can also occur by cross-linking, as will be discussed below.

Differential Scanning Calorimetry (DSC). The thermal transitions of the polymers were monitored by DSC between 0 and 240 °C with a heating and cooling rate of 20 °C/min. Glass transitions of the polymers were detected between 57 and 149 °C. No glass transition was detected for **6m**. The comparison of the glass transitions of polymers with the same flexible spacer segment but different lateral substituents at the arylenevinylene segment shows that glass transitions of **6j–l** are significantly lower than those of the phenyl-substituted **6h** (Table 6). The comparison of the polymers with the phenyl substituents at the arylenevinylene segment and different numbers of methylene units in the flexible spacers shows a discontinuous drop of the glass transition from polymers with short flexible spacers to those with long flexible spacers. The discontinuity might be due to the molecular weight range of the polymers but reflects also an odd–even effect. The polymers **6e–m** show an endothermic transition in the DSC traces of second heating runs (Table 6, Figure 1). These endotherms represent the isotropization of the LC melts, as confirmed by polarizing microscopy, with the exception of **6j–m**, since these polymers are obviously partially crystalline in contrast to **6e–i** which are amorphous.

Table 5. Characterization Data for Compounds 6

code, formula	analysis, % calcd (found) C	H	η_{inh},[a] dL/g	^{1}H-NMR chemical shifts,[b] ppm	IR spectra wavenumber, cm^{-1}	UV spectra[c] λ_{max}, nm	ϵ, mg^{-1} cm^2
6a, $C_{31}H_{22}O_4$	81.21 (80.51)	4.84 (4.59)	0.26		302 (w), 1751 (vst), 1504 (vst), 1165 (vst), 961 (st), 832 (m), 702 (st)	357	80
6b, $C_{32}H_{24}O_4$	81.34 (80.89)	5.12 (4.85)	0.14		2020 (w), 1750 (vst), 1506 (vst), 1126 (vst), 961 (m), 829 (m), 702 (m)	358	77
6c, $C_{33}H_{26}O_4$	81.46 (81.18)	5.39 (5.52)	0.57		3028 (w), 2964 (w), 1755 (vst), 1506 (vst), 1198 (vst), 1165 (vst), 1124 (vst), 962 (m), 703 (m)	358	64
6d, $C_{34}H_{28}O_4$	81.58 (81.77)	5.64 (5.83)			3032 (w), 2950 (w), 1750 (vst), 1505 (vst), 1162 (vst), 961 (st), 703 (m)		
6e, $C_{35}H_{30}O_4$	81.69 (81.00)	5.88 (6.01)	0.26		3025 (w), 2931 (w), 2862 (w), 1754 (vst), 1506 (vst), 1166 (vst), 962 (m)	354	64
6f, $C_{36}H_{32}O_4$	81.79 (82.02)	6.10 (5.99)	0.38	1.19−1.73 + 2.51 (12H), 6.77−7.47 (20H)	3035 (w), 2928 (w), 1750 (vst), 1506 (vst), 1165 (vst), 960 (m)	350	70
6g, $C_{37}H_{34}O_4$	81.89 (80.53)	6.32 (6.09)	0.11	1.36−1.71 + 2.53 (14H), 6.97−7.47 (20H)	3023 (w), 2931 (m), 2855 (w), 1756 (st), 1507 (vst), 1167 (vst), 963 (m)	358	64
6h, $C_{38}H_{36}O_4$	81.99 (81.81)	6.51 (6.39)	0.38	1.38−1.74 + 2.54 (16H), 6.97−7.50 (20H)	3032 (w), 2928 (m), 2853 (w), 1756 (vst), 1507 (vst), 1166 (vst), 963 (m)	356	62
6i, $C_{40}H_{40}O_4$	82.16 (81.76)	6.89 (7.12)	0.19	1.30−1.73 + 2.54 (20H), 6.98−7.43 (20H)	3032 (m), 2925 (vst), 2853 (st), 1753 (vst), 1507 (vst), 1168 (vst), 966 (st)	357	78
6j,[d] $C_{33}H_{31}F_3O_4$	72.25 (72.44)	5.70 (5.73)	0.19	1.28−1.72 + 2.53 (16H), 7.02−7.69 (15H)	3024 (w), 2928 (st), 2861 (m), 1760 (vst), 1506 (vst), 1166 (vst), 959 (st)	348	129
6k,[e] $C_{32}H_{31}NO_6$	73.13 (73.37)	5.95 (6.11)	0.23	1.45−1.82 + 2.62 (16H), 7.13−8.38 (15H)	3033 (w), 2995 (st), 2851 (m), 1754 (vst), 1506 (vst), 1349 (st), 1166 (vst), 962 (st)	335	44
6l, $C_{34}H_{36}O_4$	80.28 (79.88)	7.14 (7.21)	0.28	1.41−1.78 + 2.4−2.57 (22H), 7.02−7.53 (14H)	3037 (w), 2922 (vst), 2852 (m), 1756 (vst), 1506 (vst), 1166 (vst), 961 (st)	358	188
6m, C34H36O6	75.53 (75.99)	6.71 (7.14)	0.24	1.28−1.71 + 2.51 (16H), 3.85 (6H), 6.95−7.50 (14H)	3035 (w), 2928 (m), 2851 (m), 1755 (vst), 1507 (vst), 1210 (vst), 965 (m)	390, 326	64

[a] η_{inh} viscosities were measured in 1,1,2,2-tetrachloroethane at 25 °C and with a concentration of 0.5 g/dL. [b] ^{1}H-NMR spectra were measured in $CDCl_3$. [c] UV/vis spectra were measured in THF. [d] Elemental analysis for **6j** (fluorine): calcd, 10.39%; found, 10.11%. [e] Elemental analysis for **6k** (nitrogen): calcd, 2.65%; found, 2.70%.

Table 6. Thermogravimetrical Analysis, DSC, and Polarizing Microscopy of the Polymers 6a−6m

polymer	$T_{5\%}$[a] °C	T_g[b] °C	T_1[c] °C	$T_{c(microscope)}$[d] °C
6a	409	146		
6b	400	124		295 (dec)
6c	414	137		
6d	398	149		275 (dec)
6e	405	114	186	190 (dec)
6f	395	110	226	237
6g	398	60	103	86
6h	414	84	166	173
6i	404	77	179	179
6j	411	52	230	
6k	401	60	162	295
6l	330	60	137	305 (dec)
6m	406	*e*	232	

[a] $T_{5\%}$ = temperature where the sample loses 5% of its weight under a nitrogen atmosphere measured by TGA with a heating rate of 20 °C/min. [b] T_g = glass transition measured by DSC with a heating rate of 20 °C/min. [c] T_1 = endothermal transition measured by DSC with a heating rate of 20 °C/min. [d] T_c = clearing temperature, heating rate 20 °C/min. [e] T_g was not clearly detectable.

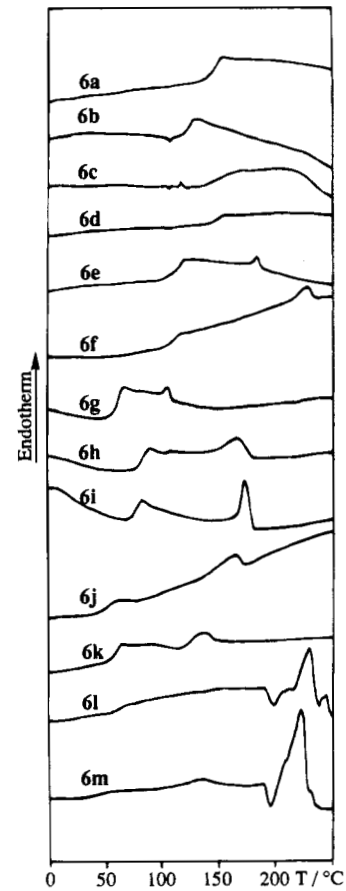

Figure 1. DSC of **6a−m** (second heating run, 20 °C/min).

Polarizing Microscopy (PM). Birefringent melts were detected by PM with polymers **6e−k**. A remarkably low clearing temperature (T_c) was detected at 86 °C for the phenyl-substituted polymer **6g** with seven methylene units. Cross-linking in the melt state at elevated temperatures has been observed with polymers containing arylenevinylene segments[1,2] and may be there as well as here attributed to cross-linking of the arylenevinylene segments. A surprising thermal stability in the melt state was observed with the CF_3-substituted polymer **6j**. Isotropization of the melt of **6j** has been observed at 295 °C by PM. It was possible to reform the mesophase upon cooling. Annealing for 3 h at 260 °C did not give any evidence for cross-linking of **6j**.

Figure 2. Microphotograph of a sample of **6j** between crossed polarizers at 262 °C at a magnification of 2773.

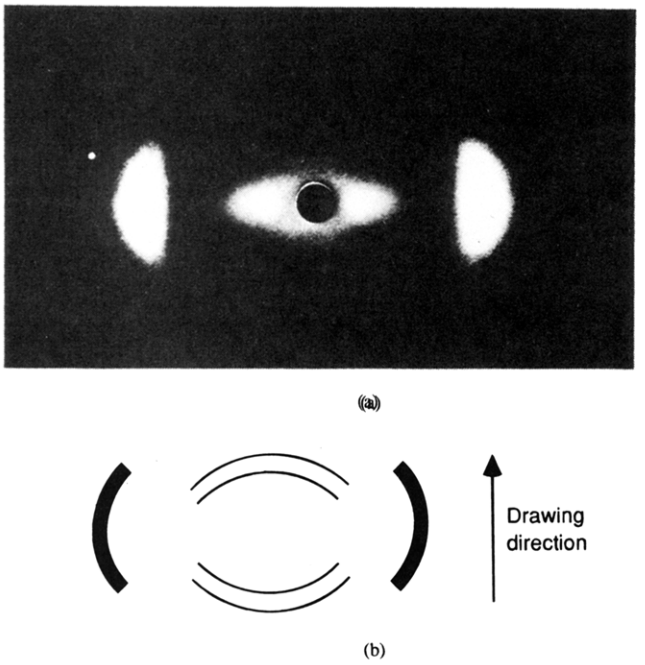

Figure 3. (a) Experimentally obtained fiber diagram (flat camera) of polymer **6i** and (b) schematic fiber diagram of polymer **6i**.

Schlieren textures were observed by PM with several of the thermotropic polymers (Figure 2), but a doubtless identification of the mesophases is not possible without corresponding X-ray investigations.

X-ray Investigations. The X-ray investigations were performed both on drawn fibers and on isotropic material in the glassy state. We will discuss, in the following, the results obtained for compound **6i** as an example.

The small angle X-ray diagram[17] of an oriented fiber shows the presence of three distinct reflections (Figure 4). They can be attributed to a layer structure and be indexed as (100), (200), and (300). The wide angle X-ray diagram reveals an amorphous halo.

Additional information is available from the fiber diagram which, however, does not display all reflections for experimental reasons. The amorphous halo is located on the equator, and the layer reflections are perpendicular to it along the meridian, i.e. along the drawing direction. The fiber diagram displays the (300) and (400) layer reflections, as shown in Figure 3. The structure displayed by compound **6i** corresponds thus

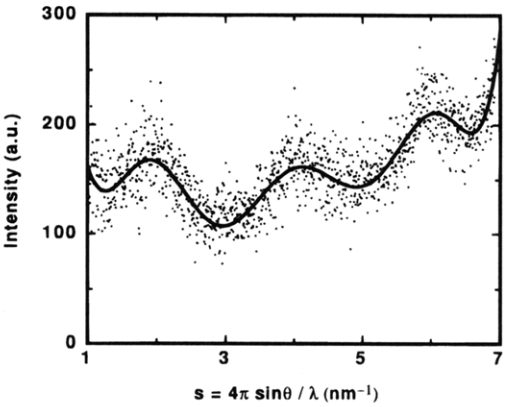

Figure 4. SAXS diagram of **6i** for a drawn fiber. (Points correspond to the experimental data, the solid line is a least squares fitted regression polynom.)

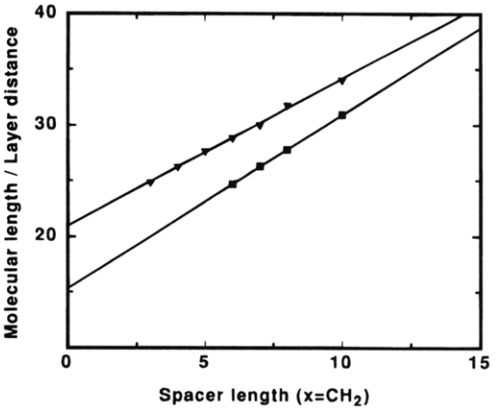

Figure 5. Experimental and simulated values for the repeat length/layer distance of **6j**−**m** (■) experiment; (▼) simulation.

Table 7. Bragg Spacing and Layer Distances of Compounds 6f−i

sample	d_{100}, Å	d_{200}, Å	d_{300}, Å	d_{400}, Å	d_{halo}, Å	d_{layer}, Å
6f			8.22		4.78	24.66
6g			8.76		4.78	26.29
6h	27.98	13.21	9.3	7.13	4.78	27.76
6i	33.14	15.23	10.35	7.82	4.78	31.48

to a smectic A phase. The narrow azimuthal widths of the reflections have to be taken as an indication of a high orientational order in the fibers.

Similar results were obtained for all compounds displaying mesophases. The layer spacing increases with increasing spacer length (Figure 5, Table 7), as expected. The unexpected finding is that the layer spacing varies by 1.56 Å per methyl unit on the average rather than by 1.26 Å, as characteristic for stretched chains. We thus have to assume that the chain configuration is not constant for all compounds. It becomes more extended with increasing spacer length. This is obvious from a comparison of the experimental data on the repeat length with those obtained from computer simulations for fully stretched chains (Figure 5). The experimental values are smaller than the ones obtained from simulations in all cases. Yet they approach the theoretical values with increasing spacer length. The extrapolation to a spacer length of zero reveals that the core is not fully elongated along the layer normal but has to be slightly tilted.

The substitution of the arylenevinylene main chains with polar substituents (compounds **6j** and **6k**) does not change the phase behavior. The polymers considered here thus display in all cases a smectic A phase as shown schematically in Figure 6.

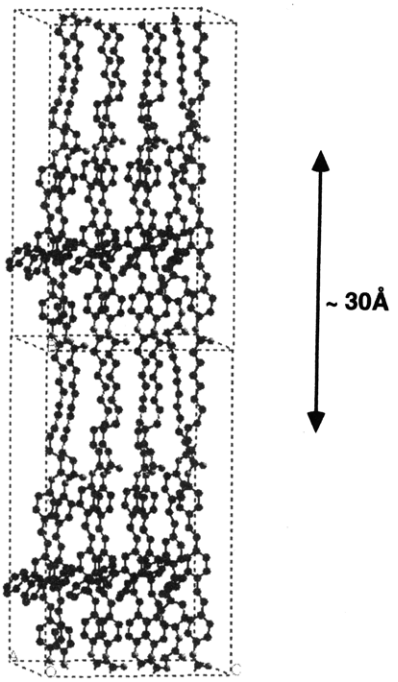

Figure 6. Model for the SA phase for **6m**.

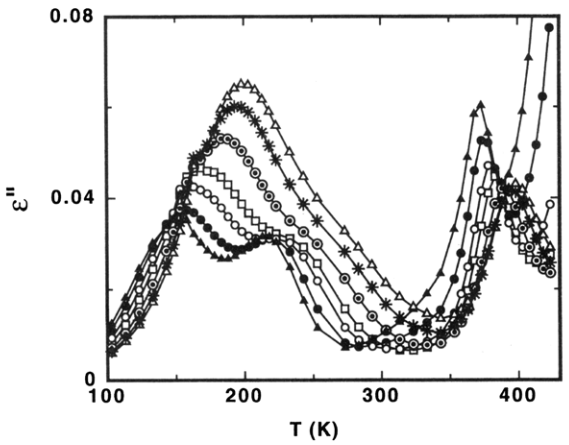

Figure 7. Dielectric relaxation of **6h** for different frequencies: (▲) 5.17×10^2 Hz; (●) 1.39×10^3 Hz; (○) 5.17×10^3 Hz; (□) 1.39×10^4 Hz; (⊙) 5.33×10^4 Hz; (*) 1.5×10^5 Hz; (△) 2.5×10^5 Hz.

Dielectric Relaxation Spectroscopy. The dielectric analysis was performed first of all to make sure that the stepwise variations of the specific heat observed via DSC measurements actually correspond to glass transitions. A second aim was to analyze the influence of the spacer length on the internal mobility.

The dielectric analysis revealed in all cases the presence of three distinct relaxation processes, as apparent from Figure 7. The high-temperature relaxation (α-relaxation) displays a high relaxation strength and a WLF behavior, as apparent from the activation diagram shown in Figure 8.

The WLF parameters $C_1 = 16$ °C and $C_2 = 53.33$ °C are close to the ones observed for amorphous polymers ($C_1 = 17.44$ °C and $C_2 = 51.6$ °C),[18,19] and the extrapolation of the glass transition temperature to low frequencies ($\nu = 0.01$ Hz) coincides with the one found by calorimetric studies (see Table 8). The results show beyond any doubt that the polymer displays a glassy smectic A phase at low temperatures.

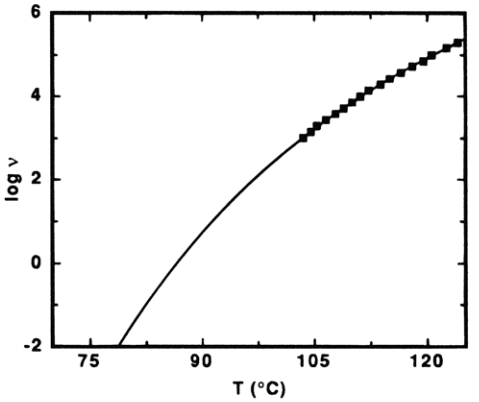

Figure 8. WLF diagram of **6h** ($C_1 = 16.0$; $C_2 = 53.33$; $T_g = 79.1$ °C).

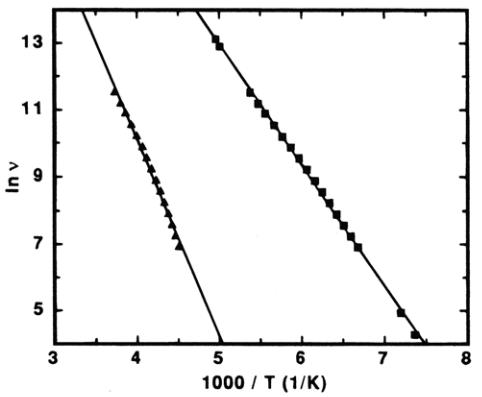

Figure 9. Arrhenius diagram (γ- and β-relaxation) of **6i**: (▲) $E_{akt(g)} = 31.12$ kJ/mol; (■) $E_{akt(b)} = 124.7$ kJ/mol.

Table 8. Activation Energies for the Low-Temperature Relaxation Processes and Glass Temperatures of 6g–k (Dielectric Spectroscopy and DSC)

sample	T_g/°C (DSC)	T_g/°C (dielectr)	$E_{akt(g)}$, (kJ/mol)	$E_{akt(b)}$ (kJ/mol)
6g	60	74	31.54	46.4
6h	84	79	30.36	80
6i	77	80	31.12	124.7
6j	52	57	32.71	
6k	60	58	31.56	

The two low-temperature β- and γ-relaxations can be attributed to secondary relaxations: they display an Arrhenius type temperature-frequency relation (Figure 9) and they possess a small relaxation strength. The lowest temperature relaxation (γ-relaxation) does not depend on the spacer length. The very small relaxation strength must be due to motions of groups with an infinitely small dipole moment. Thus the activation energy and the temperature region are typical for a crankshaft motion of the alkyl spacer. The activation energy of the β-relaxation process depends, however, quite strongly on the spacer length. We are presently not able to assign this process to a particular molecular motion.

Mechanical Test. The tensile properties of the polymers **6f** and **6i** were measured in order to get an estimate on the tensile properties of the class of polymers presented here. Fibers were drawn by pulltrusion at the temperatures stated in Table 9. The tensile properties are in the range of anisotropic

Table 9. Comparison of the Tensile Properties of 6b and 6d with Anisotropic Polyesters Reported in the Literature

polymer	modulus, GPa	tensile strength, GPa	strain at break, %
6f[a]	8.7	0.180	2.90
6i[b]	5.4	0.130	2.40
from *p*-acetoxybenzoic acid, 2,6-naphthalene dicarboxylic acid, and hydroquinone diacetate[c]	6.8	0.118	2.67
from 6-acetoxybenzoic acid, terephthalic acid, and resorcinol diacetate[d]	6.1	0.219	9

[a] Processing temperature = 180 °C. [b] Processing temperature = 155 °C. [c] Tensile properties were tested on injection molded bars.[20] [d] Tensile properties were tested on injection molded bars.[21]

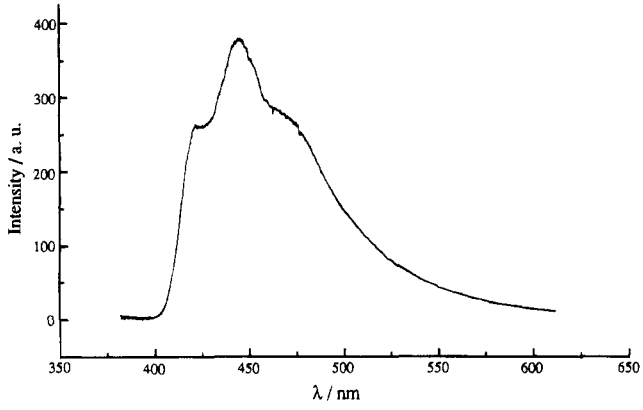

Figure 10.

polyesters without alkylene spacers in the main chain (Table 9).

Photoluminescence Spectra. The potential of polymers with arylenevinylene segments in the main chain for optical applications has been demonstrated before.[3-5]

The luminescence properties of the polymers presented here are of particular interest with respect to the combination of molecular order and light emission aiming at polarized photoluminescence and electroluminescence using higly orientated samples. Polarized photoluminescence of the polymers described here is described elsewhere.[11] As a representative example the photoluminescence spectra of **6i** is presented. **6i** exhibits blue-green light emission (λ_{ex} = 360 nm). Three distinct maxima can be detected in the time-integrated low-temperature photoluminescence spectrum of **6i**. The shape of the photoluminescence spectrum of **6i** resembles the low-temperature photoluminescence spectrum of the phenyl-substitued PPV[22] but with a significant hypsochromic shift obviously due to a shorter effective conjugation length.

Acknowledgment. The authors are indebted to Prof. Dr. W. Heitz for many helpful discussions. A generous gift of *p*-acetoxystyrene by Hoechst AG is gratefully acknowledged. This work was supported by the Fonds der Chemischen Industrie, Deutsche Forschungsgemeinschaft, and NATO.

References and Notes

(1) Martelock, H.; Greiner, A.; Heitz, H. *Makromol. Chem.* **1991**, *192*, 967.
(2) Suzuki, M.; Lim J.-C.; Saegusa, T. *Macromolecules* **1990**, *23*, 1574.
(3) (a) Yang, Z.; Sokolik, I.; Karasz, F. E. *Macromolecules* **1993**, *26*, 1188. (b) Yang, Z.; Karasz, F. E.; Geise, H. J. *Macromolecules* **1993**, *26*, 6570.
(4) v. Seggern, H.; Schmidt-Winkel, P.; Zhang, C.; Schmidt, H.-W. *Macromol. Chem. Phys.* **1994**, *195*, 2023.
(5) Hörhold, H. H.; Lux, A.; Rost, H.; Teuschel, A.; Wieduwilt, M. Presented at the Makromolekulares Kolloquium in Freiburg, 1995.
(6) (a) Bolle, B.; Greiner, A.; Heitz, W.; Mahrt, R. F.; Martelock, H. *Polym. Prepr. (Am. Chem. Soc., Div. Polym. Chem.)* **1992**, *33* (2), 378. (b) Heun, S.; Mahrt, R. F.; Greiner, A.; Lemmer, U.; Bässler, H.; Halliday, D. A.; Bradley, D. D. C.; Burns, P. L.; Holmes A. B. *J. Phys. Condens. Mater.* **1993**, *5*, 247.
(7) Oberski, J.; Bolle, B.; Schaper, A.; Greiner, A. *Polym. Adv. Technnol.* **1994**, *5*, 105.
(8) (a) Vestweber, H.; Oberski, J.; Greiner, A.; Heitz, H.; Mahrt, R. F.; Bässler, H. *Adv. Mater. Opt. Electron* **1993**, *2*, 197. (b) Lemmer, U.; Mahrt, R. F.; Wada, Y.; Greiner, A.; Bässler, H.; Göbel, E. O. *Appl. Phys. Lett.* **1993**, *62*, 2827. (c) Vestweber, H.; Sander, R.; Greiner, A.; Heitz W.; Mahrt, R. F.; Bässler, H. *Synth. Met.* **1995**, *64*, 141.
(9) Hesemann, P.; Vestweber, H.; Pommerehne, J.; Mahrt, R. F.; Greiner, A. *Adv. Mater.* **1995**, *7*, 388.
(10) Part of this work was presented at the ACS National Meeting in Denver, CO on March 28.–April 2, 1993. Greiner, A.; Hesemann, P.; Oberski, J. M. *Polym. Prepr. (Am. Chem. Soc., Div. Polym. Chem.)* **1993**, *34* (1), 176.
(11) Lüssem, G.; Festag, R.; Greiner, A.; Schmidt, C.; Unterlechner, C.; Heitz, W.; Wendorff, J. H.; Hopmeier, M.; Feldmann, J. *Adv. Mater.*, in press.
(12) Ziegler, C. B.; Heck, R. F. *J. Org. Chem.* **1978**, *43*, 2945.
(13) Chenard, B.; Manning, M. J.; Raynolds P. W.; Swenton J. S. *J. Org. Chem.* **1980**, *45*, 378.
(14) Land, H. T.; Hatke, W.; Greiner, A.; Schmidt, H.-W.; Heitz, W. *Makromol. Chem.* **1990**, *191*, 2005.
(15) Kremer, F.; Boese, D.; Meier, G.; Fischer, E. W. *Prog. Colloid Polym. Sci.* **1989**, *80*, 129.
(16) Meurisse, P.; Noel, C.; Monnerie, L.; Fayolle, B. *Br. Polym. J.* **1981**, *13*, 55.
(17) Kratky, O., Glatter, O. *Small Angle X-Ray Scattering*; Academic Press: London, 1982.
(18) Williams, M. L.; Landel, R. F.; Ferry, J. D. *J. Am. Chem. Soc.* **1955**, *77*, 3701.
(19) McCrum, N. G.; Read, B. E.; Williams, G. *Anelastic and Dielectric Effects in Polymeric Solids*; John Wiley & Sons: London, 1967; p 170.
(20) Calundann, G. W. U.S. 4,067,852, 1978.
(21) East, A. J.; Calundann, G. W., U.S. 4,318,841, 1982.
(22) Lemmer, U.; Mahrt, R. F.; Wada, Y.; Greiner, A.; Bässler, H.; Göbel, E. O. *Appl. Phys. Lett.* **1993**, *62*, 2827.

MA950723G